Philosophical Magazine

ISSN: 1478-6435 (Print) 1478-6443 (Online) Journal homepage: https://www.tandfonline.com/loi/tphm20

Polaronic transport in TiO_2 thin films with increasing Nb content

Abdullah Yildiz & Diana Mardare

To cite this article: Abdullah Yildiz & Diana Mardare (2011) Polaronic transport in TiO_2 thin films with increasing Nb content, Philosophical Magazine, 91:34, 4401-4409, DOI: 10.1080/14786435.2011.623143

To link to this article: https://doi.org/10.1080/14786435.2011.623143

Published online: 01 Nov 2011.

Philosophical Magazine
Vol. 91, No. 34, 1 December 2011, 4401–4409

Taylor & Francis
Taylor & Francis Group

Polaronic transport in TiO_2 thin films with increasing Nb content

Abdullah Yildiz[a] and Diana Mardare[b]*

[a]*Department of Physics, Faculty of Science and Arts, Ahi Evran University, 40040 Kirsehir, Turkey;* [b]*Faculty of Physics, Alexandru Ioan Cuza University, 11 Carol I Blvd., 700506 Iasi, Romania*

(*Received 4 June 2011; final version received 9 September 2011*)

The temperature dependence of the charge transport in TiO_2 films was investigated to establish the correlation between the Nb content and electrical properties. It was identified that temperature-dependent conductivity of the films is dominated by a phonon-assisted small polaron hopping model in the non-adiabatic regime. Applying the polaron hopping models of Mott, Schnakenberg and Emin to describe the observed behavior, temperature-dependent conductivity data of the films were analyzed. A detailed analysis in terms of small polaron hopping parameters in the investigated temperature regime was used to correlate electrical properties with the percentage of Nb.

Keywords: titanium oxide; thin films; electrical transport; small polaron hopping model

1. Introduction

Transition metal oxides (TMO) are of great interest due to their important electrical properties, which arise from the presence of transition metal ions (TMI) in multivalent states. These materials exhibit the formation of small polarons, and electrical conduction occurs by hopping of small polarons between ions of low and high valence states of the TMI [1–3]. Nb-doped TiO_2 (NTO) films, in particular, have received much attention since the first reports of electrical conductivity as high as 10^3–10^4 $(\Omega\,\mathrm{cm})^{-1}$ for anatase NTO films (epitaxially deposited by pulsed laser deposition) together with a high optical transmittance in the visible domain (~95%) [4,5]. These features make NTO films suitable candidates as transparent conductive oxides (TCO), since cheaper films, characterized by both high electrical conductivities and high optical transparency in the visible range, are required for different optoelectronic applications and could replace the much more expensive indium tin oxide (ITO).

Recently, we reported that small polarons play a fundamental role in determining the electrical properties of TiO_2 [6,7]. The nature of the charge carriers and the mechanism of transport in TiO_2 has been extensively investigated, but there is still no explanation that can satisfactory account for the correlation between Nb doping and the transport properties of the system in the case of small polarons formation.

*Corresponding author. Email: dianam@uaic.ro

ISSN 1478–6435 print/ISSN 1478–6443 online

http://dx.doi.org/10.1080/14786435.2011.623143
http://www.tandfonline.com

In this paper, we have investigated temperature-dependent electrical conductivity to establish the nature of the electronic transport mechanisms in TiO_2 thin films with various Nb concentrations.

2. Experimental

The films studied in this paper (undoped titania and doped with increasing Nb percentages) were obtained by the spin-coating technique. Titanium tetraisopropoxide was the source for TiO_2 and niobium pentaethoxide was the source for Nb. Both precursors were used to obtain Nb-doped materials. A mixture of 6 mL absolute ethanol and 0.5 mL titanium tetraisopropoxide was prepared under a nitrogen atmosphere. After 10 h of stirring, niobium pentaethoxide was added in increasing quantities to this mixture. Solutions with different Nb content were prepared at the following Nb/Ti. ratios: 0.08, 0.12, 0.98 and 2. To calculate the atomic ratio Nb/Ti, the volumes of titanium tetraisopropoxide $Ti(OC_4H_6)_4$ (Aldrich; 97%, 0.950 g/ml density) and niobium pentaethoxide $Nb(OC_2H_5)_5$ (Aldrich, 99.99%; 1.268 g/ml density) introduced for each sample were taken into account. Knowing the density, the quantities of Ti and Nb introduced were calculated. These quantities were then divided to the corresponding atomic masses, to obtain the number of Ti and Nb atoms. The corresponding films were deposited on unheated glass substrates by spin coating (spinner speed: 2000–3000 rotations/min). The as-deposited films were dried for 1 h at 100°C and then thermally treated in air. The heat treatment consisted in: (a) heating in air at a temperature rate of 20°C/min; (b) annealing for 1 h at 500°C; (c) cooling to room temperature in the furnace under no heating conditions. The above Nb levels are those that resulted from synthesis of the starting solutions, before heat treatment. The undoped film is designated TO, while the films with increasing Nb content are labelled NTO1, NTO2, NTO3 and NTO4.

The thin films' stucture was investigated by X-ray diffraction (XRD) using a Bruker-AXS D8 Advance, computer-controlled diffractometer (CuKα radiation, $\lambda = 1.54$ Å).

Ellipsometry studies (Horiba Jobin Yvon UVISEL VIP) revealed thickness values < 100 nm, ranging between 78 and 99 nm.

The dependence of electrical conductivity on temperature was studied in the range 300–5-70 K, using surface type cells. Thin silver films, separated by a gap of 0.8 mm, were used as electrodes.

3. Results and discussion

Representative XRD patterns for the undoped and one doped sample are presented in Figure 1. Being very thin (< 100 nm), the possible crystallization peaks are covered by the XRD pattern of the glass substrate, which is amorphous. Thus, we conclude that the studied samples are XRD amorphous.

Based on electrical conductivity data, we explored the small polaron hopping (SPH) conduction mechanism for the films [1–3]. The possibility of strong

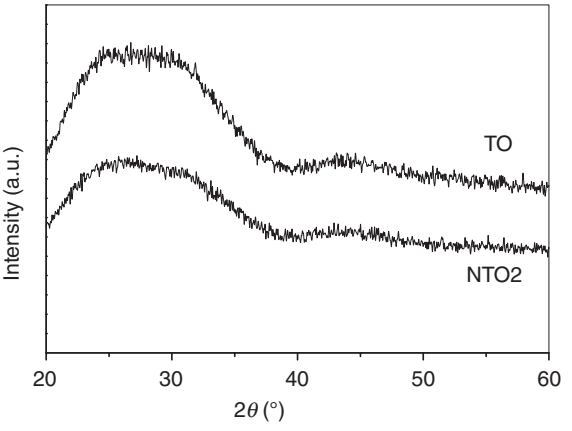

Figure 1. Representative XRD patterns for the undoped film (TO) and for one Nb-doped film (NTO2).

electron–phonon coupling and, hence, the formation of polarons are considered for the investigated films. The following relationship characterizes SPH conduction:

$$\sigma = (\sigma_0/T)\exp(-W/k_B T) \tag{1}$$

where σ_0 is the pre-exponential factor, k_B is Boltzmann's constant, and W is the activation energy, given as [8]:

$$W = W_H + W_D/2 \quad (\text{for } T > \theta_D/2)$$

and

$$W = W_D \quad (\text{for } T < \theta_D/4) \tag{2}$$

where W_H is the polaron hopping energy, W_D is the disorder energy arising from the energy difference of neighbors between two hopping sites, and θ_D is the Debye temperature.

The Debye temperature has values that are dependent on the optical phonon frequency (v_0). Therefore, it may exhibit differences according to the structural nature of the investigated material. In our previous work [6], we have used $v_0 \sim 1.11 \times 10^{13}$ Hz to estimate the values of θ_D for polycrystalline films (undoped and low Fe-doped TiO_2). However, for the present thin films, it is more realistic to obtain θ_D from Figure 2. The $\theta_D/2$ values are estimated as the temperatures where the deviations from linearity occur in the high temperature region. These values, collated in Table 1, agree well with those reported in the literature for TiO_2 [9]. More recently, Han et al. [9] found a value of 781.6 K for the Debye temperature in TiO_2, using ab initio calculations. Our experimental values of θ_D are very close to this value.

As shown in Figure 2, the temperature dependence of the electrical conductivity above $\theta_D/2$ exhibited predominantly SPH conduction. The dependence $\ln(\sigma T)$ versus $10^3/T$ is linear for $T > \theta_D/2$, while $\ln(\sigma T)$ is almost temperature-independent at low temperatures. This temperature-independent conductivity behavior at low

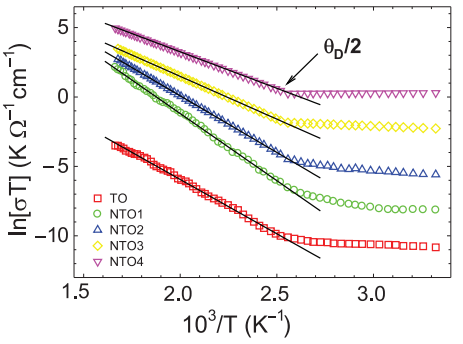

Figure 2. Plot of $\ln(\sigma T)$ versus $10^3/T$ for the films above $\theta_D/2$. The solid lines correspond to the best-fit curves with Mott's model (Equation (1)).

Table 1. Parameters obtained from the fits of Mott's model (Equation (1)) to the experimental data for the films: activation energy of electrical conduction (W), the Debye temperature (θ_D), the optical phonon frequency (v_0), the effective dielectric constant (ε_p), the polaron radius (r_p), the polaron bandwidth at 570 K (J_570 K), the value of H at 570 K (H_570 K), the SPH coupling constant (γ_p), the ratio of the polaron mass to the rigid-lattice effective mass (m_p/m^*), and the hopping carrier mobility (μ).

Sample	W (±0.01) (eV)	θ_D (K)	v_0 (Hz)	ε_p	r_p (Å)	J_570 K (meV)	H_570 K (meV)	γ_p	m_p/m^*	μ (cm^2/Vs)
TO	0.60	779.7	1.62×10^{13}	6.46	9.1	41.67	50.74	13.7	8.73×10^5	2.26×10^{-4}
NTO1	0.75	782.4	1.63×10^{13}	6.03	7.6	41.77	54.11	17.5	3.92×10^7	1.78×10^{-6}
NTO2	0.63	778.5	1.62×10^{13}	6.03	9.5	41.61	51.04	14.1	1.22×10^6	7.26×10^{-5}
NTO3	0.47	779.7	1.62×10^{13}	6.03	11.7	41.67	48.47	11.3	8.09×10^4	1.91×10^{-3}
NTO4	0.41	788.6	1.64×10^{13}	6.03	13.4	42.01	46.99	9.7	1.64×10^4	1.13×10^{-2}

temperatures is consistent with the expected behavior for small polaron hopping (SPH) conduction [1], suggesting that the polarons freeze out. We have reported similar temperature-dependent conductivity behavior for RF-sputtered TiO_2 thin films doped with small percentages of iron or niobium [6,7].

The electrical conductivity of the films increases with increasing Nb doping. For the undoped sample, the room temperature electrical conductivity (σ_{RT}) is approximately 6.6×10^{-8} $(\Omega\,cm)^{-1}$. With increasing Nb concentration, the electrical conductivity increases gradually. Overall, σ_{RT} increases by five orders of magnitude (4.5×10^{-3} $(\Omega\,cm)^{-1}$) as the Nb/Ti ratio increases from 0 to 2. It was also observed that the electrical conductivity at high temperatures increases for all films with increasing temperature, indicating temperature-dependent activation energy, W, which is a characteristic of SPH conduction mechanism in TMO.

The activation energy for electrical conduction (W), obtained from least-square fitting of the dependence $\ln(\sigma T)$ versus $10^3/T$, varied from 0.41 to 0.75 eV. The W values initially increases with Nb doping but then a decrease is observed (Table 1).

Table 2. Parameters obtained from the fits of Schnakenberg's model (Equation (3)) to the experimental data for the films: polaron hopping energy (W_H), disorder energy (W_D) and activation energy of electrical conduction (W).

Sample	W_H (±0.01) (eV)	W_D (±0.01) (eV)	W (±0.01) (eV)
TO	0.46	0.18	0.550
NTO1	0.59	0.35	0.765
NTO2	0.47	0.28	0.610
NTO3	0.38	0.19	0.475
NTO4	0.33	0.15	0.405

In light of the polaron model proposed by Schnakenberg [2], the energies W_H and W_D given in Equation (2) can be obtained. Schnakenberg [2] derived an expression for polaron conductivity for $T > \theta_D/2$. In this model, the expression for the temperature-dependent electrical conductivity has the form:

$$\sigma = \frac{\sigma_0}{T}\left[\sinh\left(\frac{h\nu_0}{k_B T}\right)\right]^{1/2} \exp\left[\left(-\frac{4W_H}{h\nu_0}\right)\tanh\left(\frac{h\nu_0}{4k_B T}\right)\right]\exp\left(-\frac{W_D}{k_B T}\right) \tag{3}$$

where h is Planck's constant and ν_0 is the optical phonon frequency, which can be estimated from the relation $h\nu_0 = k_B\theta_D$ (Table 1). The best-fit parameters, W_H and W_D, estimated using this generalized Schnakenberg's model, are given in Table 2. A good fit (solid lines in Figure 3) for the high temperature ($T > \theta_D/2$) experimental conductivity data of all the films, using Equation (3), indicates that the conduction of charge carriers is mainly governed by the SPH mechanism. The values of W, given in Table 2, are close to the values given in Table 1, obtained from the Mott's SPH model satisfying Equation (1). The values of W_H and W_D are also consistent with those of TMO films [6,7,10]. This confirms that the mechanism of electrical conductivity of the present samples could be understood by the SPH model.

To establish the correlation between Nb doping and the films' electrical properties, various polaron parameters need to be estimated for the studied films. Using the W_H values, the polaron radius (r_P) can be estimated from the following relation [11]:

$$W_H = \left(e^2/4\varepsilon_p\right)\left(r_p^{-1} - R^{-1}\right) \tag{4}$$

where R is the average spacing between the transition metal ions, given as $R \sim 2.48\, r_p$ [12]. ε_p is the effective dielectric constant given as $1/\varepsilon_p = 1/\varepsilon_\infty - 1/\varepsilon_s$ (ε_∞ and ε_s are the high and the static dielectric constant, respectively). It is expected that the ε_p values will vary slightly with the different Nb contents (it can be shown that ε_∞ has a greater influence than ε_s in determining ε_p). However, since such data are absent in the literature, we can utilize the probable values of ε_∞ and ε_s to estimate the ε_p values. We have previously reported the values of ε_s and ε_∞ as 371 (83.6) and 5.93 (6), respectively, for low Nb-doped (undoped) TiO_2 [13,14]. Using these values, ε_p is calculated (Table 1). Then, the values of r_p can be determined from Equation (4).

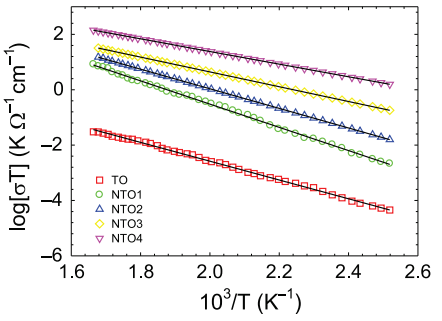

Figure 3. Plot of $\log(\sigma T)$ versus $10^3/T$ for the films above $\theta_D/2$. The solid lines correspond to the best-fit curves with Schnakenberg's model (Equation (3)).

The values of r_p are found to be consistent with the values estimated for various TMO films [6,7,10]. The r_p values, calculated from Equation (4), are given in Table 1 for the studied films. Even though the possible effect of disorder is neglected in the above calculation, the small values of the polaron radii suggest that the polarons are highly localized. Therefore, the increase in conductivity and a decrease in r_p with increasing Nb content suggests changes in localization of the polaron for the studied films.

The nature (adiabatic or non-adiabatic) of small-polaron hopping can be ascertained using the Holstein relation [8], which introduce a association between polaron bandwidth $J(T)$ and H, where

$$H(T) = (2k_B T W_H/\pi)^{1/4}(h\nu_0/\pi)^{1/2} \tag{5}$$

and evaluation of $J(T)$ can be taken from the relation [8]:

$$J(T) \approx 0.67 h\nu_0 \left(\frac{T}{\theta_D}\right)^{1/4} \tag{6}$$

In the above relations, ν_0 is estimated from the relation $h\nu_0 = k_B\theta_D$ (Table 1). If $J > H$, the SPH conduction is in the adiabatic regime. If, however, J is lower than H, the SPH conduction is in the non-adiabatic regime. In the adiabatic approach, the carrier is assumed to adjust to the instantaneous positions of the atoms. The wave function of the electron follows the nuclei and the polaron energy depends on the instantaneous position of the atoms [1–3,8,15]. In the adiabatic case, polarons are thermally activated over the potential barrier and there is a high probability of jumping to the next site. In the non-adiabatic regime, the carrier is no longer able to follow rapid fluctuations of the underlying lattice and its probability of hopping is quite small compared to the first case [1–3,8,15]. For the studied films, H varies from 46.99 to 54.11 meV (calculated at a particular temperature 570 K) and J (570 K) varies from 41.61 to 42.01 meV (see Table 1). Since $J < H$, we may conclude that the SPH conduction is in the non-adiabatic process. This is in agreement with our earlier observation from fitting the conductivity data of the Nb-doped TiO_2 films with Equation (1) [7]. We should note here that all the films fulfill the SPH conduction criterion ($J < W_H/3$) [1].

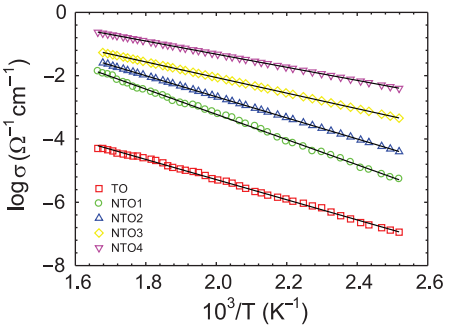

Figure 4. Plot of $\log(\sigma)$ versus $10^3/T$ for the films above $\theta_D/2$. The solid lines correspond to the best-fit curves with Emin's model (Equation (7)).

Non-adiabatic SPH conduction in the investigated films is also supported from the SPH model proposed by Emin [3]. If the interaction of the electrons with both acoustical and optical phonons is considered, the electrical conductivity for the non-adiabatic SPH conduction for $T > \theta_D/2$ is given as [3]:

$$\sigma = (Ne^2R^2/6k_BT)(J/h)^2\left[(\pi/h^2)/2(E_c^{op}+E_c^{ac})k_BT\right]^{1/2}\exp\left[W_D^2/8(E_c^{op}+E_c^{ac})k_BT\right] \times x\exp[-W_D/2k_BT]\exp\left[-E_A^{op}/k_BT - E_A^{ac}/k_BT\right] \quad (7)$$

where

$$\begin{aligned} E_c^{op} &= E_b^{op}(1/N_p)\sum_q \left[h\nu_{0,q}/2k_BT\right]\mathrm{cosech}(h\nu_{0,q}/2k_BT) \\ E_c^{ac} &= E_b^{ac}(1/N_p)\sum_q \left[h\nu_{a,q}/2k_BT\right]\mathrm{cosech}(h\nu_{a,q}/2k_BT) \\ E_A^{op} &= E_b^{op}(1/N_p)\sum_q \left[h\nu_{0,q}/2k_BT\right]^{-1}\tanh(h\nu_{0,q}/2k_BT) \\ E_A^{ac} &= E_b^{ac}(1/N_p)\sum_q \left[h\nu_{a,q}/2k_BT\right]^{-1}\tanh(h\nu_{a,q}/2k_BT) \end{aligned} \quad (8)$$

where N is the concentration of the transition metal ions given as $N = 1/R^3$, $\nu_{0,q}$ and $\nu_{a,q}$ are the optical and acoustical phonon frequencies, respectively, at wave vector q. N_p is the number of phonon modes, E_b^{op} and E_b^{ac} are the polaron binding energies related to optical and acoustical phonons, respectively. The conductivity data of the films were fitted to Equation (7) by the best fit method (Figure 4). According to the SPH model proposed by Emin [3], in calculations, we have assumed that $\nu_0 = 3\nu_a$ [3]. The values of the parameters E_b^{op}, E_b^{ac}, W_D and J, corresponding to best fits, are given in Table 3.

Although no parameters are listed in the literature as being acquired by other methods, which could be used for comparison, all the obtained hopping parameters have very probable values. These values do not differ significantly for different TMO systems. Note that the values of W_D obtained from this model, by Equation (7), are close to those obtained from Equation (3). However, the observed differences in the J

Table 3. Parameters obtained from the fits of Emin's model (Equation (7)) to the experimental data for the films: polaron binding energies related to optical phonons (E_b^{op}) and to acoustical phonons (E_b^{ac}), disorder energy (W_D) and the polaron bandwidth (J).

Sample	E_b^{op} (±0.01) (eV)	E_b^{ac} (±0.01) (eV)	W_D (±0.01) (eV)	J (meV)
TO	0.91	0.88	0.24	12.2
NTO1	0.93	0.91	0.25	27.2
NTO2	0.81	0.77	0.21	35.4
NTO3	0.53	0.41	0.19	37.1
NTO4	0.21	0.15	0.14	44.5

values obtained from Equations (6) and (7) (see Tables 1 and 3) arise from the different calculation methods. In Equation (6), J is dependent on the temperature, while, according to Equation (7), it does not depend on the temperature. On the other hand, since the values of J are still lower than the values of H, this again supports the fact that the non-adiabatic hopping conduction mechanism is valid for the investigated films.

We can now estimate other important polaron parameters. To determine the values of the SPH coupling constant γ_p, which measures carrier–phonon interactions in the films, the following relation is used [1]:

$$\gamma_p = 2W_H/h\nu_0 \tag{9}$$

One can observe that the obtained values of γ_p (given in Table 1) are higher than 4 for the investigated films; this indicates a strong carrier–phonon interaction in the films [1]. Knowing the values of γ_p, the ratio of the polaron mass (m_p) to the rigid-lattice effective mass (m^*) is estimated using the relation [1]:

$$m_p = \frac{h^2}{8\pi JR^2}\exp(\gamma_p) = m^*\exp(\gamma_p) \tag{10}$$

The huge values of m_p/m^* confirm the strong carrier–phonon interaction in the films. It is also possible to obtain the hopping carrier mobility (μ) for the investigated films. In the non-adiabatic regime, μ is described by the following equation [16]:

$$\mu = \left(\frac{eR^2}{k_BT}\right)\left(\frac{1}{\hbar}\right)\left(\frac{\pi}{4W_Hk_BT}\right)^{1/2}J^2\exp(-W/k_BT) \tag{11}$$

Using the values of J given in Table 1, as well the values of W and W_H given in Table 2, the values of μ were calculated for $T = 570$ K. The mobility is much smaller than 1 cm^2/Vs as predicted by the SPH model [1]. The values of m_p/m^* decreases and the mobility increases almost two orders when Nb doping reaches its highest value in the films.

4. Summary and conclusions

Spin coating was used to obtain the films (undoped titania, and doped with an increasing percentage of Nb) in which electrical conductivity was investigated. It has

been established that the temperature dependence of the electrical conductivity of these films, which follows the SPH conduction mechanism in the non-adiabatic regime, can be expressed according to the polaron hopping models of Mott, Schnakenberg and Emin for $T > \theta_D/2$. At low temperatures, temperature-independent conductivity behavior is observed, which is consistent with the expected behavior for small polaron hopping. We have shown that Nb content strongly influence the electrical conductivity of the investigated TiO_2 films. The various physical parameters estimated from the best fits of these models are reasonable and consistent with those in TMO systems. The increase in the Nb content leads to a decrease in the strength of electron–phonon interactions. This causes the charge carriers to move with greater mobility, leading to a dramatic increase in electrical conductivity (by five orders of magnitude), when Nb reaches its highest concentration in the films.

Acknowledgements

We thank Professor M. Girtan from Photonics Laboratory, Angers University, Angers, France, for sample preparation. This work was supported by the CNCSIS via contract no. PCCE-ID_76/2010.

References

[1] N.F. Mott, J. Non-Cryst. Solids 1 (1968) p.1.
[2] J. Schnakenberg, Phys. Status Solidi B 28 (1968) p.623.
[3] D. Emin, Phys. Rev. Lett. 32 (1974) p.303.
[4] Y. Furubayashi, T. Hitosugi, Y. Yamamoto, K. Inaba, G. Kinoda, Y. Hirose, T. Shimada and T. Hasegawa, Appl. Phys. Lett. 86 (2005) p.252101.
[5] Y. Furubayashi, T. Hitosugi, Y. Yamamoto, Y. Hirose, K. Inaba, G. Kinoda, T. Shimada and T. Hasegawa, Thin Solid Films 496 (2006) p.157.
[6] A. Yildiz, F. Iacomi and D. Mardare, J. Appl. Phys. 108 (2010) p.083701.
[7] A. Yildiz, S.B. Lisesivdin, M. Kasap and D. Mardare, Physica B 404 (2009) p.1423.
[8] I.G. Austin and N.F. Mott, Adv. Phys. 50 (2001) p.757.
[9] X.J. Han, L. Bergqvist, P.H. Dederichs, H. Müller-Krumbhaar, J.K. Christie, S. Scandolo and P. Tangney, Phys. Rev. B 81 (2010) p.134108.
[10] K.V. Ramesh and D.L. Sastry, Physica B 387 (2007) p.45.
[11] I. Jacob, R. Moreh and O. Shahal, A. Wolf, Phys. Rev. B 35 (1987) p.8.
[12] V.N. Bogomolov, E.K. Kudinev and U.N. Firsov, Sov. Phys. Solid State 9 (1968) p.2502.
[13] D. Mardare and G.I. Rusu, J. Optoelectron. Adv. Mater. 6 (2004) p.333.
[14] D. Mardare and G.I. Rusu, J. Optoelectron. Adv. Mater. 3 (2001) p.95.
[15] D. Emin and T. Holstein, Phys. Rev. Lett. 36 (1976) p.323.
[16] A. Ghosh, J. Appl. Phys. 66 (1989) p.2425.